

Experimental and Numerical Identification of a Monolithic Articulated Concentrated Strain Elastic Structure's (MACSES's) Properties

Eric L Pollard*

CSA Engineering, Inc., Albuquerque, NM 87123-3831 US

Thomas W Murphey†

Air Force Research Laboratory, Albuquerque, NM, 87117-5776 US

&

Gregory E Sanford‡

CSA Engineering, Inc., Albuquerque, NM 87123-3831 US

The objective of this research is to identify the effective continuum properties of a recently developed, deployable hierarchical truss architecture composed of carbon fiber reinforced plastic (CFRP) tubes and CFRP tape-spring hinge elements with embedded shape memory alloy (SMA) flexures; this particular structural system is referred to as monolithic articulated concentrated strain elastic structure (MACSES) and is representative of a concentrated, material deformation based deployable architecture. The scope of this study encompasses numerically and experimentally identifying the deployed stiffness and strength performance, i.e., bending, shear, torsion, and axial moduli with corresponding critical loads, of a 540 mm radius boom. Bending modulus to linear mass ratio was measured at $145 \text{ kNm}^3\text{kg}^{-1}$. Of particular interest were the sensitivity of joint composition to global properties and the acceptability of discontinuous load-paths. Developmental aspects of the MACSES architecture, including the concept at the individual element level, the packaging kinematics design, and evaluation and scaling the global performance of the system are reported in a preceding manuscript.

I. Introduction

DEPLOYABLE, monolithic architectures customarily require members to comply to a packaged configuration, compromising stiffness and incurring mass penalties for strength to accommodate reduced volume states.¹ The merit of the monolithic articulated concentrated strain elastic structure (MACSES) predecessor concept was demonstrating how non-mechanically, stowable trusses, composed of piece-wise constant cross-section elements, can maintain strength-stability and stiffness properties competitive with conventional mechanically jointed, articulating trusses assembled from uniform high-stiffness composite members. The aforementioned piece-wise constant cross-section elements were synthesized of structurally efficient, high-stiffness composite for the majority of their length and a less structurally efficient, more compliant material and geometry at either end of the span.² This philosophy leads to monolithic systems packaged through concentrated, material deformation of hinge regions which have no dead-band and can exploit stored strain energy to motivate self-reconfiguration relevant to deployable space applications. Additionally, the forerunning concept debuted a kinematic design with the ability to collapse and expand structural hierarchy throughout a one-, two-, or three-dimensional truss network. Comprehensive experimental evaluations and parallel, numerical modeling predictions to distill representative beam

* Engineer, CSA Engineering, Inc., 1451 Innovation Pkwy. SE Suite 100, Albuquerque, NM 87123-3831 US, AIAA Member

† Research Aerospace Engineer, Space Vehicles Directorate, 3550 Aberdeen Ave. SE, Albuquerque, NM 87117-5776 US, AIAA Senior Member

‡ Project Engineer, CSA Engineering, Inc., 1451 Innovation Pkwy. SE Suite 100, Albuquerque, NM 87123-3831 US, AIAA Member

Report Documentation Page

Form Approved
OMB No. 0704-0188

Public reporting burden for the collection of information is estimated to average 1 hour per response, including the time for reviewing instructions, searching existing data sources, gathering and maintaining the data needed, and completing and reviewing the collection of information. Send comments regarding this burden estimate or any other aspect of this collection of information, including suggestions for reducing this burden, to Washington Headquarters Services, Directorate for Information Operations and Reports, 1215 Jefferson Davis Highway, Suite 1204, Arlington VA 22202-4302. Respondents should be aware that notwithstanding any other provision of law, no person shall be subject to a penalty for failing to comply with a collection of information if it does not display a currently valid OMB control number.

1. REPORT DATE APR 2007	2. REPORT TYPE	3. DATES COVERED 00-00-2007 to 00-00-2007	
4. TITLE AND SUBTITLE Experimental and Numerical Identification of a Monolithic Articulated Concentrated Strain Elastic Structure's (MACSES's) Properties		5a. CONTRACT NUMBER	
		5b. GRANT NUMBER	
		5c. PROGRAM ELEMENT NUMBER	
6. AUTHOR(S)		5d. PROJECT NUMBER	
		5e. TASK NUMBER	
		5f. WORK UNIT NUMBER	
7. PERFORMING ORGANIZATION NAME(S) AND ADDRESS(ES) Air Force Research Laboratory, Space Vehicles Directorate, 3550 Aberdeen Ave. SE, Albuquerque, NM, 87117-5776		8. PERFORMING ORGANIZATION REPORT NUMBER	
9. SPONSORING/MONITORING AGENCY NAME(S) AND ADDRESS(ES)		10. SPONSOR/MONITOR'S ACRONYM(S)	
		11. SPONSOR/MONITOR'S REPORT NUMBER(S)	
12. DISTRIBUTION/AVAILABILITY STATEMENT Approved for public release; distribution unlimited			
13. SUPPLEMENTARY NOTES 48th AIAA/ASME/ASCE/AHS/ASC Structures, Structural Dynamics, and Materials Conference, 23 - 26 April 2007, Honolulu, Hawaii			
14. ABSTRACT			
15. SUBJECT TERMS			
16. SECURITY CLASSIFICATION OF:			17. LIMITATION OF ABSTRACT Same as Report (SAR)
a. REPORT unclassified	b. ABSTRACT unclassified	c. THIS PAGE unclassified	
			18. NUMBER OF PAGES 10
			19a. NAME OF RESPONSIBLE PERSON

properties are particularly insightful to such a structural system which is modular and may deviate from a true truss-like response. Rigorous interrogation of a high fidelity, repetitive element readily enables analytical trades to strategically allocate system structural and control requirements to responsively field a platform with lean deployed performance margins.

A. Concept

This truss concept is a recently developed, deployable hierarchical architecture composed of carbon fiber reinforced plastic (CFRP) tubes and CFRP tape-spring hinge elements with embedded shape memory alloy (SMA) flexures. The composite longerons and battens communicate via the tape-spring elements with unique joints to enable the hinges to each fold about a single axis between a stowed configuration and the operational topology; the joints dictate the tape-spring bend radius and consequently the strain realized (Fig. 1). In order to minimize the bend radius for increased compaction efficiency, a less structurally efficient material system and geometry is utilized for the hinge regions at the extremes of the elements while a more efficient and less compliant material system is utilized throughout the majority of the structure. It may not be intuitive this pairing of structural roles leads to greater mass efficiency as well. Increasing in hierarchy the non-mechanically joined longerons and battens form four-longeron trusses junctioning at hub bays to serve as members in a one-dimensional truss network or formatted in two-dimensions, resulting in a grillage. The former variant is particularly suited for precision, kilometer-scale booms and the latter shallow structural format would serve as a photovoltaic or radar array platforms. These repetitive elements can be further formatted in three-dimensions.

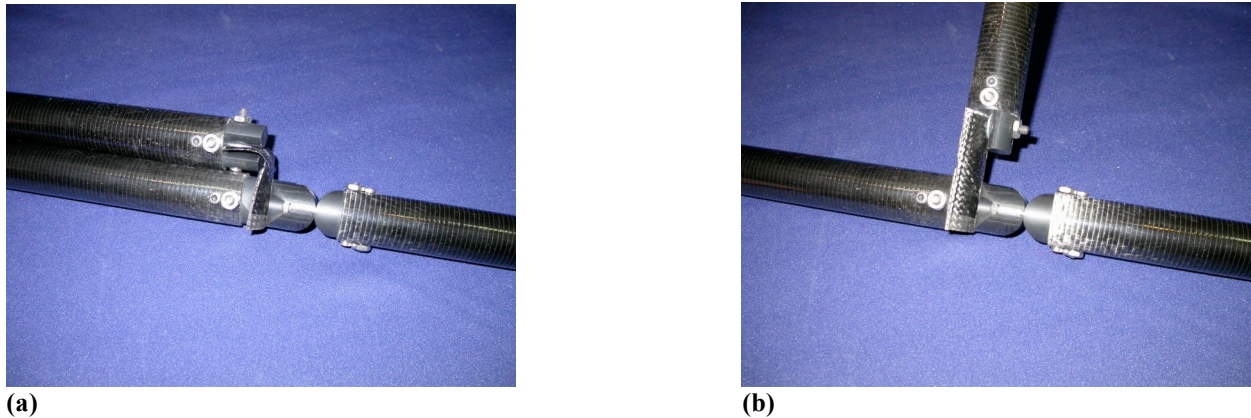
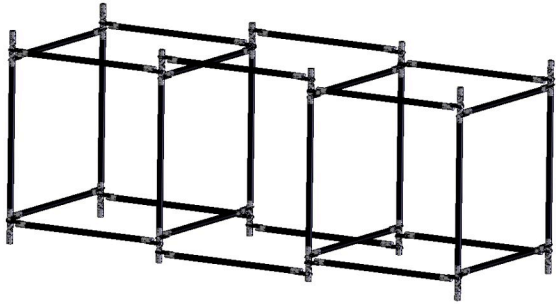


Fig. 1 The composite longerons and battens communicate via the tape-spring elements with unique joints to enable the hinges to each fold about a single axis between a, (a) stowed configuration; (b) and the operational topology.

The tape-spring hinge axes are deliberately oriented to enforce the kinematics design. To package the concept, several truss bays are simultaneously sheared in one direction to collapse their length with an increase in height followed by shearing the hub bays and finally, simultaneously shearing both the truss bays and hub bays again. The first packaging stage is similar to the movement of the Pactruss design as described in Refs. 3-5. Four-captured MACSES reconfiguration events depict an abbreviated three-bay model and prototype at each stage of the sequence, (i) an expanded truss bay disposed between two-, expanded hub bays, (ii) the truss bay sheared to collapse this assembly against the faces of the hub bays, (iii) the first hub bay shear substantially collapsing the structure into a planar topology, and (iv) the last stage, the simultaneous second hub bay shear and the second truss bay shear substantially collapsing the structure into a linear topology (Fig. 2). With some creativity, one can extrapolate how this pattern propagates through a two-dimensional format. This kinematic design is also valid for greater hierarchy booms or arrays with some depth where the movement of the two grillages forming opposite faces would mimic the two-dimensional sequence and the batten elements connecting these two faces would participate in the final two-stages. Linear compaction ratios of 400:1 and volumetric compaction ratios of 2,000:1 are reasonable.



(a)



(b)



(c)



(d)



Fig. 2 Four-captured MACSES reconfiguration events depict an abbreviated three-bay model and prototype at each stage of the sequence, (a,b) (i) an expanded truss bay disposed between two-, expanded hub bays, (c,d) (ii) the truss bay sheared to collapse this assembly against the faces of the hub bays, (e,f) (iii) the first hub bay shear substantially collapsing the structure into a planar topology, (g,h) and (iv) the last stage, the simultaneous second hub bay shear and the second truss bay shear substantially collapsing the structure into a linear topology.

B. Background

There are limited documented efforts in the literature to thoroughly experimentally investigate deployable structures suited for the class of expected loads and requirements Hedgepeth⁶ describes. Some notable examples locate points of fidelity within the design space which can drift from theoretical expectations.⁷⁻⁹ These examples mature the structural sciences and limit unreconciled models and intuition alone from guiding the designer. Augmenting the population of empirically analyzed point designs across representative deployable architecture topologies will enable judicious survey of existing and proposed concepts. Further, this exercise will erode uncertainty in the relative culpability of such factors as model reduction, fabrication imprecision, and test fixture misalignment, traceable to the disparity between expected and measured structural responses.

C. Objective

The objective of this research is to identify the effective continuum properties of the MACSES hierarchical truss concept, a concentrated, material deformation based deployable architecture. The scope of this study encompasses numerically and experimentally identifying the deployed stiffness and strength performance, i.e., bending, shear, torsion, and axial moduli with corresponding critical loads, of a 540 mm radius boom. Of particular interest were the sensitivity of joint composition to global properties and the acceptability of discontinuous load-paths.

II. Experimental and Numerical Identification

A. Model

Numerical identification of the effective continuum stiffness and strength-stability response of a fixed-free supported 540 mm radius, 45.0° diagonal angle, four-longeron, and three-bay MACSES boom, comparable to the test article, was performed on a tie constrained finite element (FE) model assembled from tube, tape-spring hinge element, and various joint component instances occurring in the joint assemblies (Fig. 3a). In contrast to the test article, the FE model does not capture the fastener details of the prototyped joint assemblies which would understandably need to be bonded, not bolted, for the network to be truly monolithic. The 25.4 mm diameter tubes and 12.7 mm radius tape-springs, subtending 150° with integrated SMA flexures, are CFRP laminates whereas the prototyped joint components are extruded solids (Table 1). This model is capable of 0.814% volumetric compaction realizing 1.11% maximum hinge strain. Rigid endplate boundary conditions were emulated by defining two-rigid bodies on either end of the boom's primary axis with which each respective set of joint assemblies participates at the appropriate tape-spring hinge interfaces. Full-integration shell elements assigned with composite section definitions represented the laminates at a global seed size of 2.00 mm and lamina material constants were consistent with experimental results of the IM7/977-2 system.¹⁰ In order to investigate the sensitivity of joint composition to global properties, the joint component instances were modeled with the baseline, as tested, ABS plastic and a more mass efficient material system, Ti-6Al-4V. Tetrahedral continuum elements assigned with isotropic section definitions represented the joint components at a global seed size of 2.00 mm and Young's modulus and Poissons ratio pair constants were assumed to be 2.00 GPa, 0.350 and 114 GPa, 0.342, for ABS plastic and Ti-6Al-4V, respectively. The resiliency of the baseline 2.24 m and 5.53 kg truss and the truss with Ti-6Al-4V joints at 11.7 kg were identified employing the ABAQUS Standard finite element code's static solver and negative pivot loads were determined employing the ABAQUS Standard finite element code's subspace eigensolver.¹¹ (Mass tallies do not include fasteners found on the test article.)

To address the acceptability of discontinuous load-paths, a MACSES design feature which allows for tape-spring nesting at a joint assembly to increase packaging efficiency and which may be necessary when the hinge arc centers are located within the joint volumes, an individual hinge-tube-hinge element was freed from the assembled FE model and numerically identified. Responses of interest included axial stiffness, 1.07 MNm², and pinned-pinned strength, 556 mN. Then based on these properties, theoretical approximations were made of global stiffness and strength for a continuous load-path, four-longeron MACSES system through analytical expressions of true truss-like behavior.¹²

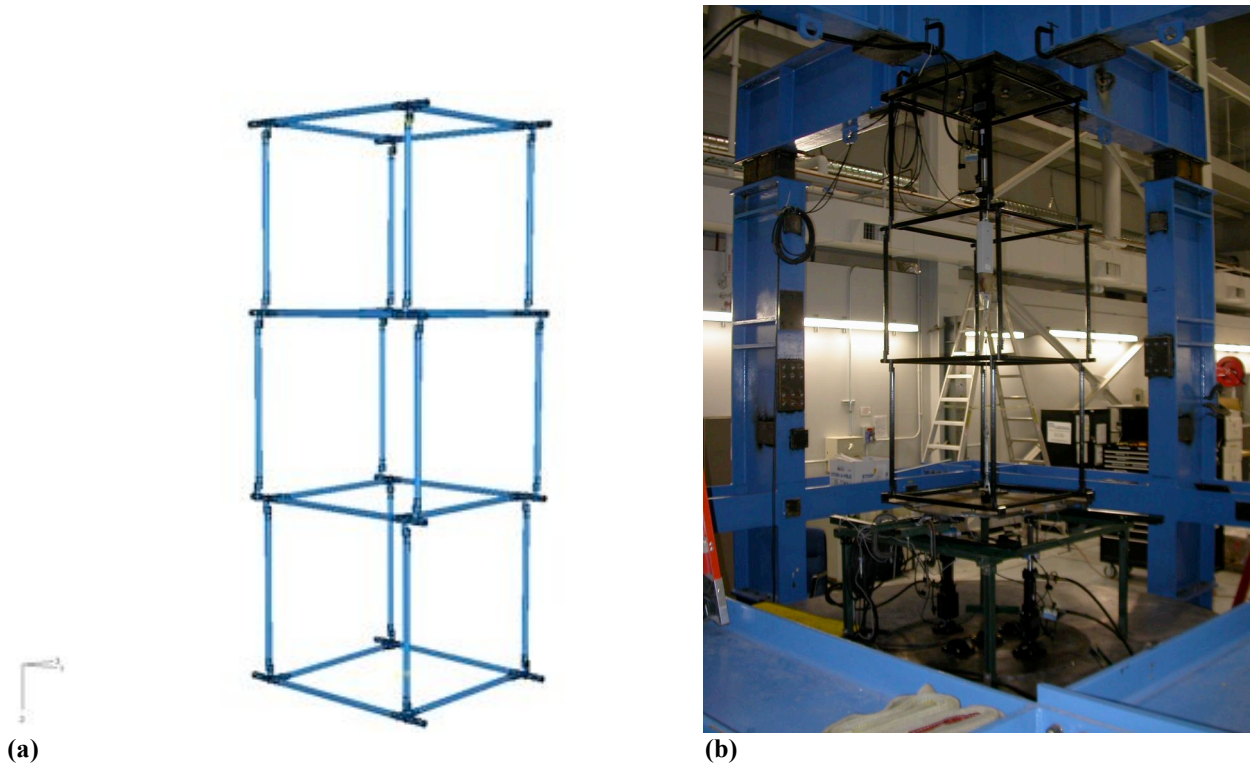


Fig. 3 (a) Numerical identification of the effective continuum stiffness and strength-stability response of a fixed-free supported 540 mm radius, 45.0° diagonal angle, four-longeron, and three-bay MACSES boom, comparable to the test article, was performed on a tie constrained finite element (FE) model assembled from tube, tape-spring hinge element, and various joint component instances occurring in the joint assemblies. (b) Experimental identification of the three-bay MACSES test article followed encastre mounting the top of the truss, oriented parallel to gravity, to a reaction structure and a fixedly attaching a plate at the opposing free end to serve as a proxy for the modeled rigid body and to accommodate various actuator and sensor configurations to affect and measure the article.

Table 1 The 25.4 mm diameter tubes and 12.7 mm radius tape-springs, subtending 150° with integrated SMA flexures, are CFRP laminates.

Laminate	Lamina	Material	Thickness	Orientation
tube	1	IM7/977-2	1.52 mm	0°
tape-spring hinge	1	IM7/977-2	200 μm	±45°
	2 (two, 1.47 mm width wires positioned along longitudinal edges)	Nitinol	305 μm	N/A
	3	IM7/977-2	200 μm	±45°

B. Test Setup

Experimental identification of the three-bay MACSES test article followed encastre mounting the truss, oriented parallel to gravity, to a reaction structure and a fixedly attaching a plate at the opposing free end to serve as a proxy for the modeled rigid body and to accommodate various actuator and sensor configurations to affect and measure the

article (Fig. 3b). The free end plate was off-loaded with an active tether at its center of gravity for all load cases; this tether was servo-hydraulically load controlled with a 7.12 kN actuator and a 1.33 kN capacity load cell rated at 0.08% full scale precision. An array of 12.7 mm range linear variable displacement transducers, rated at 0.35% full scale non-linearity, oriented parallel and transverse to the boom's primary structural axis, probed the plate to detect compliance. Transversely oriented transducers were paired with an opposing dead channel transducer to negate the influence of the probes' 2.45 N preload.

Bending load cases were performed with an additional pair of servo-hydraulically load controlled assemblies, with identical actuators to the off-load channel, but mated to 8.90 kN capacity load cells rated at 0.08% full scale precision. These assemblies were pinned-pinned mounted between the free end plate and the base of the reaction structure to form a symmetric couple about the article's geometric center at a 305 mm radius. Shear and torsion load cases were performed with a linear actuator via a tether acting normal to gravity and through a 97.9 N capacity load cell, rated at 0.08% full scale precision, to the free end plate center and at a 229 mm radius or moment arm from the center, respectively. Axial load cases were performed with the active off-load channel. The bending and torsion load case configurations relied on laser sight located actuator and end plate mounts to vertically align the boom, where as the axial and shear load case configuration did not include a vertical alignment design element at the free end. A free axle disposed between the base of the reaction structure and the free end plate center served as such element for the torsion load cases. Loads were engaged incrementally with sine waveform step profiles.

C. Results

Agreement between the experimentally evaluated, effective continuum stiffness and strength-stability properties exhibited by the fixed-free supported three-bay MACSES boom test article and FE predictions vary by load case between 3.1% and 88.5% for compliance and between 23.3% and 229.0% for elastic stability (Tables 2 and 3). Bending force was assumed as the average of the two load cell channels; transverse displacement values used to calculate the reported compliances were taken as the average value of two live transducers located near the perimeter of the free end plate and 180° apart. A discussion on the corrections made for the off-load restoring force follows. Complications with vertical alignment of the test article invalidated the axial load cases.

Table 2 Effective continuum stiffness properties as predicted with FE models, evaluated experimentally, and approximated analytically.

Property	FE Model	Test Article	Ti-6Al-4V Joint FE Model	Continuous Load-Path Analytical Model
Bending modulus	41.4 kNm ²	359 kNm ²	814 kNm ²	624 kNm ²
shear modulus	303 N	2.61 kN*	530 N	
torsion modulus	400 Nm ²	413 Nm ²	10.2 kNm ²	
axial modulus	236 kN		2.97 MN	4.28 MN

*corrected for off-load restoring force

Table 3 Effective continuum strength-stability properties as predicted with FE models, evaluated experimentally, and approximated analytically.

Property	FE Model	Test Article	Ti-6Al-4V Joint FE Model	Continuous Load-Path Analytical Model
bending strength	431 Nm	131 Nm	1.59 kNm	600 mNm
shear strength	48.8 N	63.6 N*	60.0 N	
torsion strength	82.2 Nm	29.1 Nm	630 Nm	
axial strength	262 N		500 N	2.22 N

*corrected for off-load restoring force

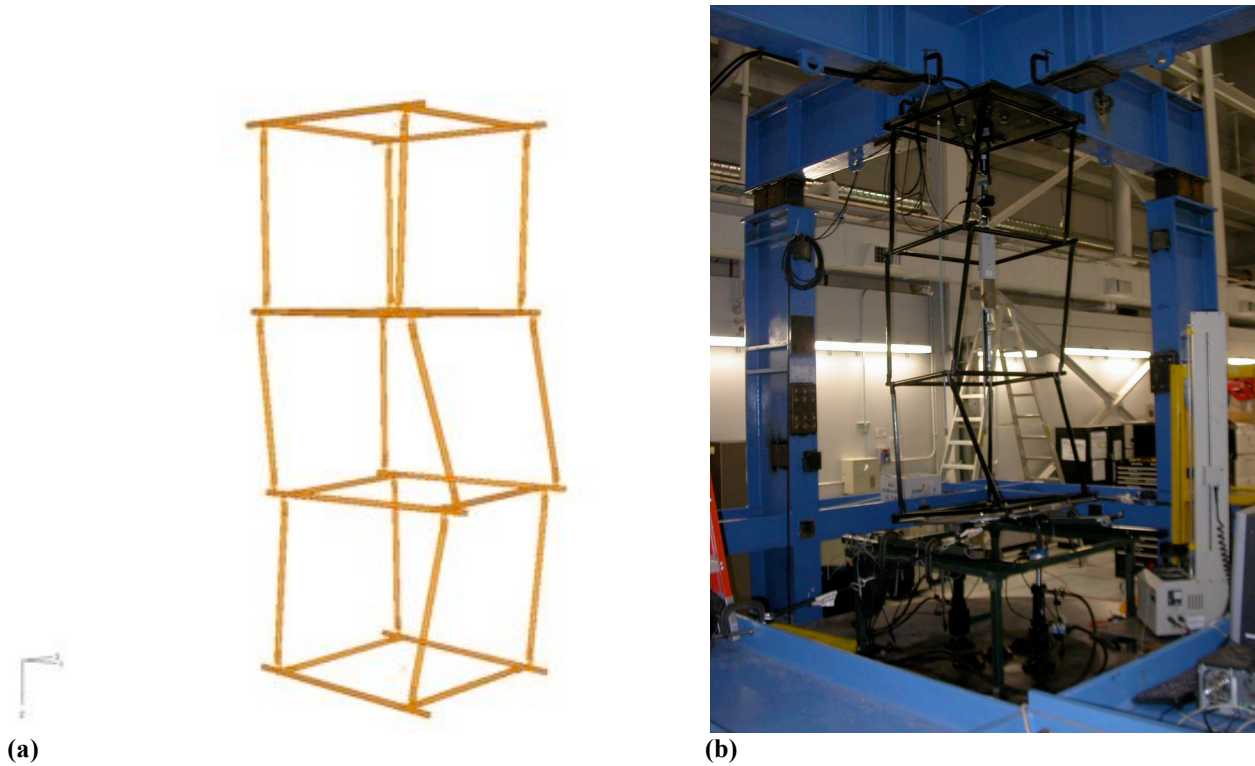


Fig. 4 (a) FE modeled bending, buckling mode of the three-bay MACSES boom. (b) Experimentally observed bending, buckling mode of the three-bay MACSES test article.

D. Error Analysis

Instrumentation confidence intervals can be determined for this investigation based on the appropriate load cell and displacement sensor ratings. Load cell precision was taken as the summation of static error band and non-linearity contributors. Confidence intervals, expressed in the corresponding property dimensions, were figured for each load case conservatively assuming load cell precision extremes and worst-case transducer non-linearity accumulation was realized over the data considered for identification. The shear stiffness confidence interval is not compounded by bending stiffness uncertainty (Table 4).

Table 4 Confidence intervals, expressed in the corresponding property dimensions, were figured for each load case.

Property	Bending	Shear	Torsion	Axial
stiffness	$\pm 43.8 \text{ kNm}^2$	$\pm 38.9 \text{ N}$	$\pm 7.51 \text{ Nm}^2$	N/A
strength	$\pm 4.34 \text{ Nm}$	$\pm 78.3 \text{ mN}$	$\pm 17.9 \text{ mNm}$	N/A

Corrections must be made in the recorded force for the shear load cases to account for the off-load restoring force. This measurement contamination arises as the test article's free end is displaced off vertical center and the off-load channel, commanded to maintain the weight force of the free end plate at 658 N, projects a force component in a direction transverse to the boom's primary structural axis (Fig. 5). Transverse force data was post processed to remove the contamination.

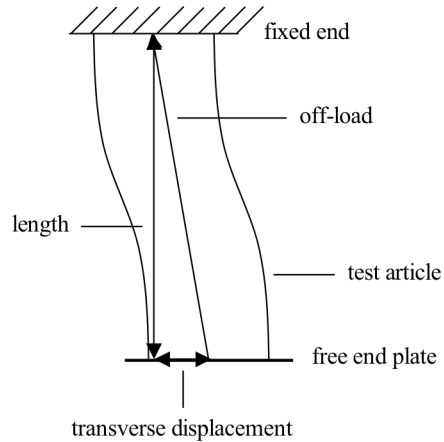


Fig. 5 Corrections must be made in the recorded force for the shear load cases to account for the off-load restoring force.

III. Discussion

This research identified the effective continuum properties of a recently developed, deployable hierarchical truss architecture composed of CFRP tubes and CFRP tape-spring hinge elements with embedded SMA flexures; this particular structural system is referred to as MACSES and is representative of a concentrated, material deformation based deployable architecture. The scope of this study encompassed numerically and experimentally identifying the deployed stiffness and strength performance, i.e., bending, shear, torsion, and axial moduli with corresponding critical loads, of a 540 mm radius boom. Bending modulus to linear mass ratio was measured at $145 \text{ kNm}^3\text{kg}^{-1}$.

Disagreement between the general resiliency of the test article and theoretical, numerical model is most probably attributable to the infidelity of not capturing fastener details in the joint assemblies of the FE representation. Considering any force transmission through the prototype, both tube and tape-spring hinge stiffness and strength performance is disproportionate to the ABS plastic joint components. Comparisons between the appreciable property gains of the Ti-6Al-4V joint FE model and baseline predictions further highlight the sensitivity of the structure to joint parameters. Following this explanation, one would expect the discrepancy between the stiffness of the test article and baseline numerical predictions to be proportional to the improvement of the Ti-6Al-4V joint FE model. This was not so for the shear and torsion load cases. Suspected of aliasing the true shear response was the loss of off-load as the structure deflects transversely, effectively pre-loading the article, i.e., the complimentary projection of the off-load force onto the gravity vector of the free end plate decreases as the off-load restoring force increases; intuitively, the tape-spring hinges oriented to fold in an equal sense manner would dominate the transverse compliance and tensioning these elements would be expected to throw the measured shear stiffness. Inspection of the hinge interfaces upon torsion loading the article suggested bolted joint compliance was culpable for the exceptional lack of torsional stiffness. The resiliency penalty paid for tape-spring nesting at a joint assembly to increase packaging efficiency, resulting in discontinuous load-paths, can be entirely recovered by increasing the modulus of the joint material.

This MACSES variant clearly responds drastically different than a true truss and the continuous load-path analytical model strength values are only reported for completeness. The test article had a tendency to torque upon transverse loading and the measured shear strength-stability was achieved with additional constraints to maintain the targeted deformation pattern. The latter value closely approaches the Ti-6Al-4V joint FE model critical shear load as one would expect since stiffening the joint components will refocus strain energy to the tape-spring hinges and global shear stability will be ultimately paced by the local stability of these elements.

Acknowledgments

Funding for this research was provided by the Air Force Research Laboratory Space Vehicles Directorate and monitored by Dr. Jeffry S Welsh. The authors are grateful for the expertise and support of the directorate's modeling and composites laboratories.

References

- ¹*Deployable Structures*, Edited by S Pellegrino, CISM Courses & Lectures, CISM, 2001.
- ²Pollard, EL, Murphey, TW, & Mejia-Ariza, JM, "Development of Concentrated Strain Based Deployable Truss Structures," *Proceedings of the 47th AIAA/ASME/ASCE/AHS/ASC Structures, Structural Dynamics, & Materials Conference*, 2006-1682, AIAA, Washington, DC, US, 2006.
- ³Von Roos, A & Hedgepeth, JM, "Design, Model Fabrication, & Analysis for a Four-Longeron, Synchronously Deployable, Double-Fold Beam Concept," AAC-TN-1139, Astro Aerospace Corp., 1985.
- ⁴Hedgepeth, JM, "Pactruss Support Structure for Precision Segmented Reflectors," NASA CR-181747, 1989.
- ⁵Mikulas, MM, Lou, MC, Withnell, PR, & Thorwald, G, "Deployable Concepts for Precision Segmented Reflectors," JPL D-10947, 1993.
- ⁶Hedgepeth, JM, "Critical Requirements for the Design of Large Space Structures," NASA CR-3484, 1981.
- ⁷Crawford, RF, "Investigation of a Coilable Lattice Column," NASA CR-1301, 1969.
- ⁸Hinkle, JD, Warren, P, & Peterson, LD, "Structural Performance of a Gossamer Isogrid Column with Initial Geometric Imperfections," *Proceedings of the 42nd AIAA/ASME/ASCE/AHS/ASC Structures, Structural Dynamics, & Materials Conference*, 2001-1682, AIAA, Washington, DC, US, 2001.
- ⁹Hinkle, JD, Peterson, LD, & Warren, PA, "Structural Performance of an Elastically Stowable Tubular Truss Column," *Proceedings of the 43rd AIAA/ASME/ASCE/AHS/ASC Structures, Structural Dynamics, & Materials Conference*, 2002-1555, AIAA, Washington, DC, US, 2002.
- ¹⁰Welsh, JS & Wegner, PM, "The Effect of Adhesive Bond Thickness and Material Type on Structure Stiffness," *Proceedings of the 43rd AIAA/ASME/ASCE/AHS/ASC Structures, Structural Dynamics, and Materials Conference*, 2002-1726, AIAA, Washington, DC, 2002.
- ¹¹*ABAQUS/Standard User's Manual*, Hibbitt, Karlsson, & Sorensen, Inc., 2006.
- ¹²*Recent Advances in Gossamer Spacecraft*, Edited by CHM Jenkins, Progress in Astronautics & Aeronautics, AIAA, Washington, DC, 2006.